EFFECT OF BILEAFLET MECHANICAL VALVE MALFUNCTION ON BLOOD HEMODYNAMICS

Othman Smadi (1), Marianne Fenech (2), Ibrahim Hassan (1), Lyes Kadem (1)
1. Concordia University, Montreal, Canada; 2. Ottawa University, Ottawa; Canada

INTRODUCTION

Stenosis or incompetence at severe levels reduce the performance of the heart and place additional stress and strain upon it. Therefore, in many cases, surgical replacement of the diseased valve with a Bioprosthetic or Mechanical Heart Valves (MHV) is necessary to restore valve function. Although the lifelong anticoagulant medication and the possible clinical complications (e.g. blood elements damage and/or thrombus formation), Bileaflet MHV are the most implanted valves with over 170,000 implants worldwide each year as a result of high durability and appropriate characteristics for blood hemodynamics (in terms of low pressure gradient and low shear stress level)[1]. Unfortunately, in some cases, Thromboembolic complications and/or pannus formation are possible after Bileaflet valve implantation. The mortality percentage for the reoperation might be as high as 69%. By the way, even though the low percentage of the deficiency in one or both leaflets(0.2%-6% per patient-year), the dangerous of leaflet malfunction as life threatening event leads us to pay attention to the clinical complication that will accompany this problem. [2]

Recently, computational Fluid Dynamics (CFD) came into view as a robust tool in arterial blood flow studies. While the majority of numerical simulations of blood flow through aortic MHV have been conducted based on laminar flow assumption [3, 4 and 5], recently have studies begun to explore turbulent or transitional blood flow through MHV. In order to find the onset of turbulence in physiological pulsatile flow, Peacock et al. [6] studied experimentally the pulsatile fluid flow in a straight tube and concluded that the critical Reynolds number is correlated to Strouhaul Number (St) as well as to Womersley parameter (α). Moreover, the disturbed aortic flow was predicted.

Although the laminar-transitional-turbulent natures of blood flow through the MHV, the Wilcox's low-Reynolds $\kappa-\omega$ model was able to predict the laminar and transitional as will as the turbulent periods of the blood flow through stenosed artery [7, 8]. In addition, by conducting experimental and numerical study, Wilcox's low-Reynolds $\kappa-\omega$ was found to be adequate for modeling blood flow through Bileaflet Valves [9].

To address the remarkable change in blood hemodynamics and consequence clinical complications and to emphasis the importance of early detecting of the problem, the realistic pulsatile physiological blood flow through the defected valve was simulated in normal function and in various states of malfunction by using commercial software (Fluent 6.3.26 - Fluent Inc.; Lebanon; NH; USA) and adapting transitional $\kappa-\omega$ turbulence model. Dramatic changes in turbulent shear stress level and vortex formation and shedding and high value of wall shear stress were observed during the simulation.

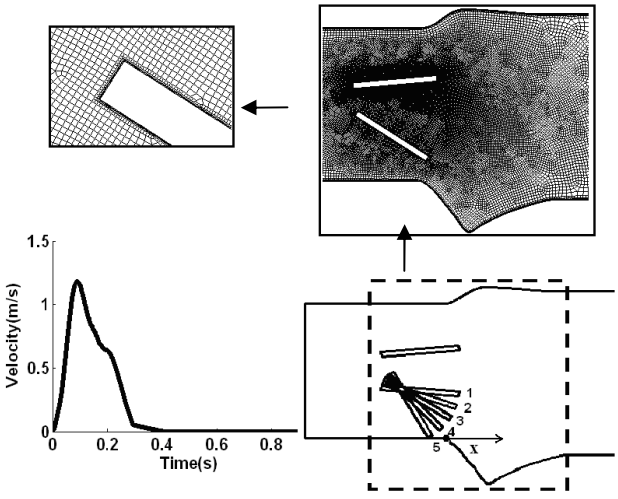

Figure 1: Model geometry for the five different cases; 1) 0% malfunction; 2) 25% malfunction; 3) 50% malfunction; 4) 75% malfunction; 5) 100% malfunction. (Mesh quality for the sinuses and leaflets is also shown).

NUMERICAL METHOD

Five 2D models were created in the current study. The only lower leaflet was moved from fully opened position (85°; 0% malfunction) to fully closed position (30°; 100% malfunction) with three equally spaced

intermediate angles of 71.25° (25% malfunction), 57.5° (50% malfunction) and 43.75° (75% malfunction). As shown in Figure (1) non symmetric sinuses were modeled based on the in vivo study performed by [10] and used in vitro by [11]. For the upstream and downstream sections, the lengths were 10D and 4D, respectively. The bileaflet mechanical valve was modeled based on a 25 mm St. Jude Medical Hemodynamic Plus valve. Therefore, the inner diameter was 22.3mm. The hinge mechanism of the valve has been neglected and this valve has been chosen since it is the most commonly implanted clinically. It should be noted that the current study focuses only on one blocked leaflet, since this case is more complex to be detected when compared to the case where both leaflets are blocked [2]

Time-averaging or Reynolds averaging has been used as a means of analyzing turbulence by separating fluctuating properties with their time-mean values. Thus, the true velocity is defined by $u_i = \overline{u}_i + u'_i$, where the overbar refers to time-average and prime refers to fluctuation from this average, when this is substituted in the general Navier-stokes equation, a new term will be introduced, i.e., the Reynolds stresses ($-\rho\overline{u'_i u'_j}$). To close the governing equations with the new extra variables, in present study, two-equation transitional $\kappa-\omega$ model was used through which The Reynolds stress is approximated using The Boussinesq relation for incompressible flow [12]

$$-\rho\overline{u'_i u'_j} = \mu_t\left(\frac{\partial u_i}{\partial x_j}+\frac{\partial u_j}{\partial x_i}\right)-\frac{2}{3}\left(\rho k+\mu_t\frac{\partial u_i}{\partial x_i}\right)\delta_{ij} \quad (1)$$

where u_i is the average velocity in i direction and μ_t is the turbulent eddy viscosity and k is the turbulent kinetic energy. Using Transitional k-w model, the eddy viscosity is modeled as

$$\mu_t = \alpha^*\left(\frac{\rho k}{\omega}\right) \quad (2)$$

where ω is the specific dissipation rate and α^* is the low-Re correction factor which is computed from

$$\alpha^* = \alpha^*_\infty\left(\frac{\alpha^*_0+\mathrm{Re}_t/R_k}{1+\mathrm{Re}_t/R_k}\right) \quad (3)$$

where $\mathrm{Re}_t = \rho k/\mu\omega$, R_k=6, $\alpha^*_0 = \beta_i/3$, $\beta_i = 0.072$ and α^*_∞ = 1. k and ω are solved by two-equation k-w model

$$\rho\frac{\partial(k)}{\partial t}+\rho u_j\frac{\partial}{\partial x_j}(k)=\frac{\partial}{\partial x_j}\left((\mu+\sigma^*\mu_t)\frac{\partial k}{\partial x_j}\right)-\rho\overline{u'_i u'_j}\frac{\partial u_i}{\partial x_j} - \rho\beta^* f_{\beta^*} k\omega \quad (5)$$

$$\rho\frac{\partial(\omega)}{\partial t}+\rho u_j\frac{\partial}{\partial x_j}(\omega)=\frac{\partial}{\partial x_j}\left((\mu+\sigma\mu_t)\frac{\partial \omega}{\partial x_j}\right)-\rho\overline{u'_i u'_j}\frac{\partial u_i}{\partial x_j}(\alpha\frac{\omega}{k}) - \rho\beta\, f_\beta\,\omega^2 \quad (6)$$

where $\sigma^* = \sigma = 0.5$ and β =0.09 .

For k-equation, β^* and f_{β^*} are given by

$$\beta^* = \beta^*_\infty\left(\frac{4/15+(\mathrm{Re}_t/R_\beta)^4}{1+(\mathrm{Re}_t/R_\beta)^4}\right) \quad (7)$$

$$f_{\beta^*} = \begin{cases} 1 & \chi_k \le 0 \\ \dfrac{1+680\chi^2{}_k}{1+400\chi^2{}_k} & \chi_k > 0 \end{cases} \quad (8)$$

where β^*_∞ = 0.09, R_β=8 and $\chi_k \equiv \frac{1}{\omega^3}\frac{\partial k}{\partial x_j}\frac{\partial \omega}{\partial x_j}$

For w-equation, α and f_b are given by

$$\alpha = \frac{\alpha_\infty}{\alpha^*}\left(\frac{\alpha_0+\mathrm{Re}_t/R_\omega}{1+\mathrm{Re}_t/R_\omega}\right) \quad (9)$$

$$f_\beta = \frac{1+70\chi_\omega}{1+80\chi_\omega} \quad (10)$$

where α_∞ =0.52, R_ω=2.95 , α_0 =1/9, $\chi_\omega = \left|\frac{\Omega_{ij}\Omega_{jk}S_{ki}}{(\beta^*{}_\infty\omega)^3}\right|$

where $\Omega_{ij} = \frac{1}{2}(\frac{\partial u_i}{\partial x_j}-\frac{\partial u_j}{\partial u_i})$ and $S_{ij} = \frac{1}{2}(\frac{\partial u_j}{\partial x_i}+\frac{\partial u_i}{\partial u_j})$.

In present work, two dimensional, pulsatile and turbulent blood flow through bileaflet valve was simulated. The cardiac output was considered 5 L/min and heart rate of 70 bpm. We considered the common values for density and dynamic viscosity which were equal to 1000 kg/m3 and 0.0035 kg/m.s respectively

Typical Physiological cardiac cycle was consederd as inlet condition Fig (1) and ambient pressure was considered as outlet condition.

Steady flow conducted first to establish the grid density. Moreover, additional care was made close from the wall and leaflets surfaces to maintain (y+ << 1). Time step was reduced to 0.25 ms where the results did not vary by reducing more the time step and only 10-20 iterations were required for convergence. Finally, as we did not consider the fluid-structure interaction between the leaflets and fluid and even though the simulation was conducted for the whole cardiac cycle, only the period of simulation from the fully opening leaflet's instant in the acceleration part of the systolic phase (65ms) to the instant when the valve starts closing in the deceleration part of systolic phase (250ms) was investigated.

RESULTS AND DICUSSION

As shown in figure (2), by increasing the percentage of malfunction, the blood flow becomes laterally instead of being both centrally and laterally as in the healthy model. More over, the maximum velocity value in the entire field increases significantly and become as high as 3.6 m/s when the lower leaflet is 100% defected (completely closed). In turn, the differences in velocity magnitudes through the three valve orifices will disturb the flow down stream of the valve figure (3).

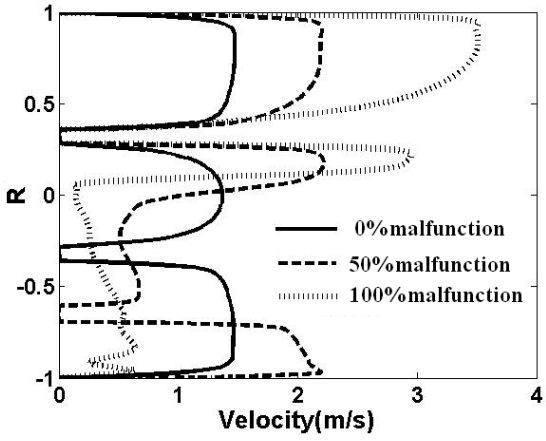

Figure 2: Velocity profiles at the vicinity of the valve at the peak for different malfunctions.

As shown in figure (3), in healthy model, vortices occur around the upper and lower leaflets. As the flow rate increases, a vortex is shed from the leaflets and a vortex wake develops. In the sinus, a vortex also noticed and a single vortex ring was noticed During the deceleration phase the vortex shedding phenomenon still exist with creating second major vortex ring in the sinus area. In the mean time, in the defected models the flow became more complex and a new vortex rings were created in different areas of the domain. More over, in the 50% malfunction, during the deceleration phase the sinus vortex vanished and new vortices were shown down stream of the valve. In the mean time when the malfunction reached the maximum (100%), a new vortex was created behind the defected valve in the side of he left ventricle aortic tract.

However, by creating a vortical flow down stream of the valve, the residential time for the blood elements in relatively high shear stress regions down stream of the valve will increase and the potential of platelet activation and/or red blood cells damage will be highly exist [9].

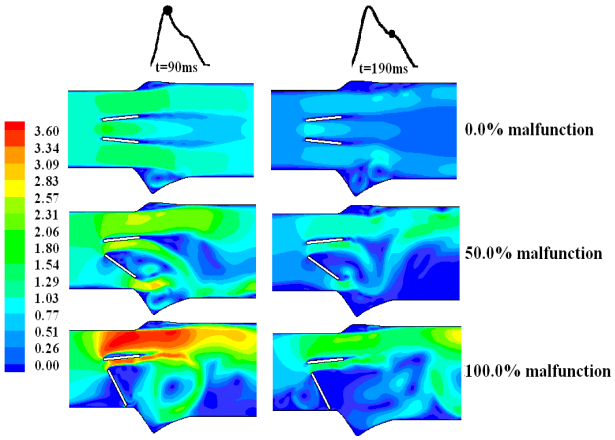

Figure 3: Velocity contours for different malfunctions at the peak and 100 ms after the peak.

Wall Shear Stress (WSS) at the lower wall close from the vicinity of the valve is shown in figure 4. WSS is proportional to the percentage of malfunction and reached the maximum (750 Pa) when the leaflet was completely closed. Moreover, in 100% malfunction the maximum WSS was shifted upstream of the valve where the valve housing covers the aortic wall therefore the high shear stress level might not affect the aortic wall. In contrast, WSS is shifted slightly downstream of the valve which may affect the endothelial cells in the sinus wall.

Wall shear stress about 40 N/m^2 might damage the endothelial cells and higher value around 100 N/m^2 could wash away the endothelial cells. As a result the blood will be in direct contact with subendothelial connective tissue. In contrast to endothelial cells, the deposition of blood elements and thrombotic material will occur on subendothelial tissue of defected wall. It

is important to point out that the level of shear stress that will affect the red blood cells is lower when the red blood cells are adhered to the wall [14].

As shown in figure 5, turbulent shear stress level and position will change in the case of defected valve. In 50% malfunction of the lower leaflet, the relatively high shear stress areas covered most of the domain down stream of the valve and the maximum value (156 Pa) was found toward the lower leaflet. In the mean time, in case of completely defected valve the turbulent shear stress reached as high as 189 Pa and the high turbulent shear stress areas were found through the upper orifice and down stream of the valve close from the upper wall. Although the threshold of turbulent shear stress to create red blood cells damage is higher than the calculated on, the potential of blood hemolysis still exist as there are other factors like exposure time and shear exposure history relevant to blood hemolysis [13])

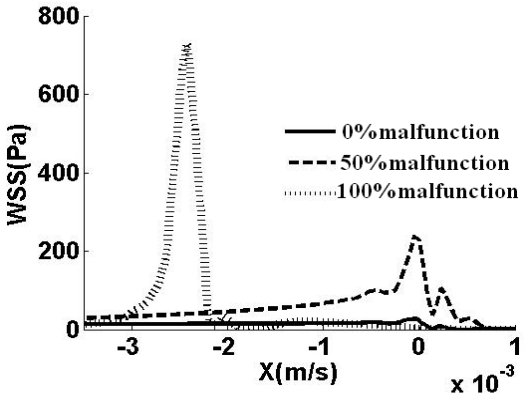

Figure 4: Wall shear stress at the peak for different malfunctions.

Finally, in present study, dramatically, the turbulent shear stress and wall shear stress in addition to vortices formation are affected by the severity of valve malfunction. By other words, the thrombus formation rate is higher as the severity is higher. And early detection to the problem will give a better chance to solve the problem and save the patient life.

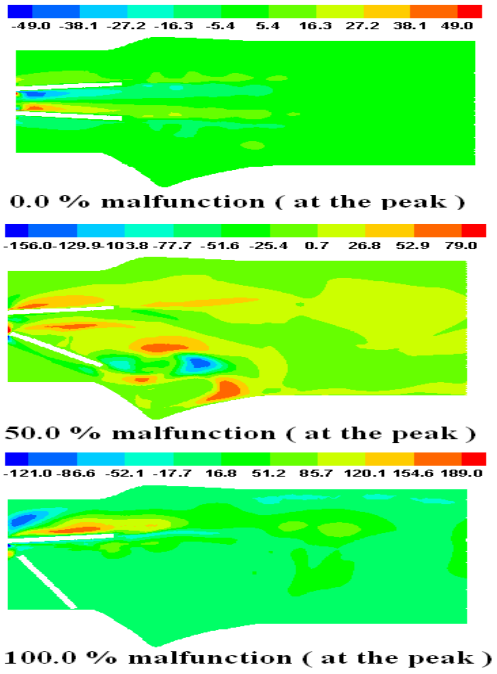

Figure 5: Turbulent shear stress at the peak for different malfunctions.

REFERENCES

[1] A. P. Yoganathan, K. B. Chandran and F. Sotiropoulos, " Flow in Prosthetic Heart Valves: State-of-the-Art and Future Directions, "Annals of Biomedical Engineering, vol. 33(12), pp. 1689–1694, 2003.

[2] P. Montorsi, D. Cavretto, M. Alimento, M. Muratori and M. Pepi, "Prosthetic mitral valve thrombosis: can fluoroscopy predict the efficacy of thrombolytic treatment?" Circulation vol. 108, pp.79-84, 2003.

[3] M. Grigioni, C. Daniele, C. Gaudio , U. Morbiducci, G. D'Avenio and V. Barbaro,"Three-Dimensional numerical simulation of flow through an aortic bileaflet valve in a realistic model of aortic root," American Society for Artificial Internal Organs, vol. 51(3), pp.176-183, 2005.

[4] L. Ge, S. C. Jones, F. Sotiropoulos, T. M. Healy and A. P. Yoganathan,"Numerical simulation of flow in mechanical heart valves: grid resolution and the assumption of flow symmetry," Journal of Biomechanical Engineering, vol. 125, pp.709-719, 2003.

[5] C. Guivier, V. Deplano and P. Pibarot, "New insights into the assessment of the prosthetic valve performance in the presence of subaortic stenosis through a Fluid-Structure interaction model," Journal of Biomechanics, vol. 40(10), pp.2283-2291, 2007.

[6] J. Peacock, T. Jones, C. Tock and R. Lutz, "The onset of turbulence in physiological pulsatile flow in a straight tube," Experiments in Fluids, vol. 24, pp. 1-9, 1998.

[7] F. Ghalichi and X. Deng,"Turbulence detection in a stenosed artery bifurcation by numerical simulation of pulsatile blood flow using the low-Reynolds number turbulence model," Biorheology, vol. 40, pp. 637-654, 2003.

[8] J. Straatman and D. Steinman,"Two-equation turbulence modeling of pulsatile flow in a stenosed tube," Journal of Biomechanical engineering, vol. 126, pp.625-635, 2004.

[9] D. Bluestein, E. Rambod and M. Gharib,"Vortex shedding as a mechanism for free emboli formation in mechanical heart valves," Journal of Biomechanical Engineering, vol. 122, pp.125-134, 2000.

[10] H. Reul, A. Vahlbruck, M. Giersiepen, T. H. Schmitz-Rode, V. Hirtz and S. Effert,"The geometry of the aortic root in health, at valve disease and after valve replacement," Journal of Biomechanics, vol.23 (2), pp.181-190, 1990.

[11] M. Grigioni, C. Daniele, G. D'Avenio and V. Barbaro, "The influence of the leaflets' curvature on the flow field in two bileaflet prosthetic heart valves," Journal of Biomechanics, vol. 34, pp.613-622, 2001.

[12] D. C. Wilcox, Turbulence modeling for CFD, 2nd edition, DCW Industries, La Canada, California,1998.

[13] M. V. Kameneva, G. W. Burgreen, K. Kono, B. Repko, J. F. Antaki and M. Umezo, "Effect of turbulent stresses upon mechanical hemolysis: experimental and computational analysis" ASAIO J, vol. 50, pp.418-423, 2004.

[14] A. P. Yoganathan, W. H. Corcoran and E. C. Harrison," Wall shear stress measurements in the near vicinity of prosthetic aortic hear valves," Journal of Bioengineering, vol. 2, pp.369-379, 1978.